# Two-dimensional wave-current interactions in presence of a submerged structure
## (没水構造物のある場合の二次元波・流れの相互干渉)


| | | |
|---|---|---|
| S. Mokudai | Student Member | Department of Civil Engineering, Nagasaki University |
| M. Mohiuddin | Student Member | School of Marine Science and Engineering, Nagasaki University |
| H. Togashi | Fellow Member | Department of Civil Engineering, Nagasaki University |
| Y. Hirayama | | Department of Civil Engineering, Nagasaki University |


## 1 Introduction

Frequent wave-current interactions take place near the coastal or nearshore areas. In real situations, variations in water depths and current velocities around a submerged structure make the interactions more complex than usual. Because wave transformation around a submerged structure involves combined wave refraction and diffraction phenomena. A two-dimensional numerical model based on Madsen type (Madsen *et al.*, 1992) extended Boussinesq equations is developed for wave transformation analyses in a wave-current coexistence field where a submerged structure is placed on the flat sea bottom.

## 2 Theoretical formulation

The depth-integrated extended Boussinesq equations (Madsen *et al.* 1992) are as follows:

$$\frac{\partial S}{\partial t}+\frac{\partial P}{\partial x}+\frac{\partial Q}{\partial y}=0; \qquad P=\int_{-h}^{S} u\,dz \quad , \qquad Q=\int_{-h}^{S} v\,dz \tag{1}$$

$$\begin{aligned}&\frac{\partial P}{\partial t}+\frac{\partial}{\partial x}\left(\frac{P^2}{d}\right)+\frac{\partial}{\partial y}\left(\frac{PQ}{d}\right)+gd\frac{\partial S}{\partial x}-\left(B+\frac{1}{3}\right)h^2\left(\frac{\partial^3 P}{\partial x^2\partial t}+\frac{\partial^3 Q}{\partial x\partial y\partial t}\right)-Bgh^3\left(\frac{\partial^3 S}{\partial x^3}+\frac{\partial^3 S}{\partial x\partial y^2}\right)\\&-h\frac{\partial h}{\partial x}\left(\frac{1}{3}\frac{\partial^2 P}{\partial x\partial t}+\frac{1}{6}\frac{\partial^2 Q}{\partial y\partial t}+2Bgh\frac{\partial^2 S}{\partial x^2}+Bgh\frac{\partial^2 S}{\partial y^2}\right)-h\frac{\partial h}{\partial y}\left(\frac{1}{6}\frac{\partial^2 Q}{\partial x\partial t}+Bgh\frac{\partial^2 S}{\partial x\partial y}\right)=0\end{aligned} \tag{2}$$

$$\begin{aligned}&\frac{\partial Q}{\partial t}+\frac{\partial}{\partial x}\left(\frac{PQ}{d}\right)+\frac{\partial}{\partial y}\left(\frac{Q^2}{d}\right)+gd\frac{\partial S}{\partial y}-\left(B+\frac{1}{3}\right)h^2\left(\frac{\partial^3 Q}{\partial y^2\partial t}+\frac{\partial^3 P}{\partial x\partial y\partial t}\right)-Bgh^3\left(\frac{\partial^3 S}{\partial y^3}+\frac{\partial^3 S}{\partial x^2\partial y}\right)\\&-h\frac{\partial h}{\partial y}\left(\frac{1}{3}\frac{\partial^2 Q}{\partial y\partial t}+\frac{1}{6}\frac{\partial^2 P}{\partial x\partial t}+2Bgh\frac{\partial^2 S}{\partial y^2}+Bgh\frac{\partial^2 S}{\partial x^2}\right)-h\frac{\partial h}{\partial x}\left(\frac{1}{6}\frac{\partial^2 P}{\partial y\partial t}+Bgh\frac{\partial^2 S}{\partial x\partial y}\right)=0\end{aligned} \tag{3}$$

Here, $u$ and $v$ are particle velocities in $x$- and $y$-direction respectively, $d$ is the total water depth, $h$ is the water depth, $S$ is the surface fluctuation, $g$ is the acceleration due to gravity, $P$ and $Q$ are depth-integrated velocity components (fluxes) in $x$- and $y$-direction respectively, and $B$ (=1/15) is a curve fitting parameter.

The wave-current dispersion relation for the governing equations is as Eq. (4) (Mohiuddin *et al.*, 1999). In this equation, $\omega$ is the absolute wave angular frequency ($=2\pi/T$), $T$ is the absolute wave period, $k$ is the wave number, and $U$ is the current velocity in the $x$-direction (an equivalent uniform current).

$$\frac{C^2}{gh}=\frac{CU}{gh}\left\{\frac{1-k^2h^2(B+1/3)}{1+k^2h^2(B+1/3)}\right\}+\frac{1}{gh}\left\{\frac{U^2+gh\left(1+Bk^2h^2\right)}{1+k^2h^2(B+1/3)}\right\}-\frac{U}{C}\frac{1}{gh}\left\{\frac{U^2-gh\left(1+Bk^2h^2\right)}{1+k^2h^2(B+1/3)}\right\} \tag{4}$$

## 3 Numerical computations

Governing equations are solved by the finite difference technique. In the scheme, Boussinesq correction terms – *Sxxx*, *Syyy*, *Sxyy*, and *Syxx* – are included implicitly as surface curvatures and these curvatures are computed by the method of cubic spline. $S$ is calculated by the explicit way, and $P$ and $Q$ are computed by the implicit technique. In each direction, the finite difference approximation of equation of motion reduces to a tridiagonal matrix. And this matrix is solved by the double sweep algorithm.

## 4 Computational conditions

The model is applied to a domain, which is 26m×26m in size. The still water depth in the domain is 0.6m and on the top of the structure is 0.4m. In numerical simulations, the incident wave period is 2.2s and the incident wave height is 0.1m. Computations are performed for the following cases: (1) waves without a current field ($U$=0m/s), (2) waves with following currents ($U$=0.25m/s), and (3) waves with adverse currents ($U$=-0.25m/s). Here, variations in currents are introduced along the $x$-axis only. Both the normally and the obliquely incident wave propagation are considered. In the study, adverse and following currents signify flow velocities in the negative $x$-direction and the positive $x$-direction respectively; the distances (in meters) along the $x$-axis and the $y$-axis can be obtained by multiplying a factor equal to 0.5.

## 5 Results and discussions

For normal wave propagation ($\theta$=0°) on $x$-directional following currents, computed instantaneous surface fluctuations, wave heights and mean water levels (set-down) distribution are shown in Figs. 1(a), 1(b) and 1(c) respectively. In a particular region of the domain, wave profiles (Fig. 1a) and wave heights (Fig. 1b) are larger than the surrounding ones. Furthermore, larger wave heights are found beyond the submerged structure in the wave propagation direction instead over the top of it. The drop of mean water level (set-down) is greater over the structure and the maximum drop is found for waves on adverse currents (Figs. 1c & 2b). Wave heights (Fig. 2a) and mean water levels (Fig. 2b) distribution are compared along the sections $x$=41 and $x$=27 respectively. Figure 2(a) shows that adverse currents modify the maximum wave height and the side lobes significantly. However, following currents have less influence on it. Oblique wave propagation ($\theta$=15°) on adverse currents is simulated and computed results for surface fluctuations and wave heights distribution are shown in Figs. 3(a) and 3(b) respectively.

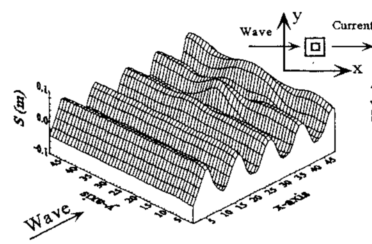


Fig. 1(a): Surface profiles ($U$=0.25m/s).

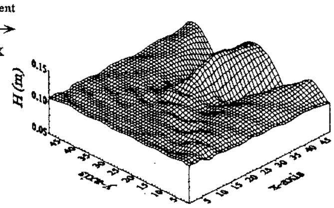


Fig. 1(b): Wave heights ($U$=0.25m/s).

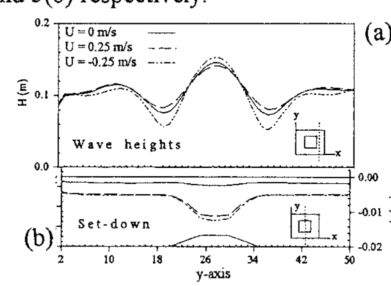


Fig. 2: (a) $x$=41, (b) $x$=27

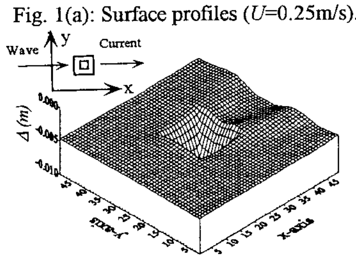


Fig. 1(c): Set-down ($U$=0.25m/s).

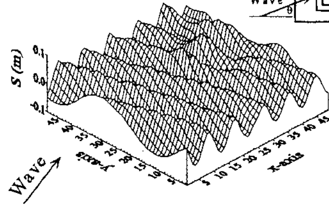


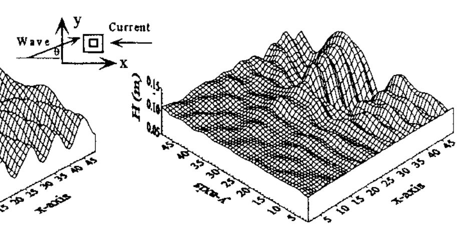


Fig. 3(a): Surface profiles ($U$= -0.25m/s). Fig. 3(b): Wave heights ($U$= -0.25m/s).

## 6 Conclusions

A wave-current numerical model is presented for wave characteristic analyses in presence of a submerged structure in the domain. The model is applied for both adverse currents and following currents, and simulations are conducted for normal and oblique wave propagation. For normally incident wave propagation, computed results show that adverse currents modify wave properties around the structure significantly. However, following currents have comparatively less impact on wave characteristics.

## References

Madsen, P. A. and O. R. Sørensen (1992): A new form of the Boussinesq equations with improved linear dispersion characteristics. Part 2. A slowly-varying bathymetry, *Coast. Engrg.*, Vol. 18, pp. 183-204.

Mohiuddin, M., H. Togashi and Y. Hirayama (1999): Modeling wave-current interactions over a sloping bottom topography, *Proc. Coast. Engrg.*, JSCE, Vol. 46, pp. 71-75 (in Japanese).